International Journal of Solids and Structures 45 (2008) 5165–5180

Contents lists available at ScienceDirect

International Journal of Solids and Structures

journal homepage: www.elsevier.com/locate/ijsolstr

Homogenization problems of a hollow cylinder made of elastic materials with discontinuous properties

George Chatzigeorgiou [a], Nicolas Charalambakis [a,*], Francois Murat [b]

[a] Institute of Mechanics of Materials, Division of Structures, Department of Civil Engineering, Aristotle University of Thessaloniki, Thessaloniki GR 541 24, Greece
[b] Laboratoire Jacques-Louis Lions, Université Pierre et Marie Curie, Boîte courrier 187, 75252 Paris Cedex 05, France

ARTICLE INFO

Article history:
Received 12 March 2008
Received in revised form 7 May 2008
Available online 3 June 2008

Keywords:
Multilayered tube
Homogenization
Dissimilar anisotropic materials
Laminated composites

ABSTRACT

In this paper, we present the homogenization of an anisotropic hollow layered tube with discontinuous elastic coefficients. We focus on some aspects of technological importance, such as the effective coefficients of anisotropic materials, the behavior of the homogenized displacements and stresses, the discontinuities of in-plane shear, hoop and longitudinal stresses, the homogenization-induced anisotropy in the isotropic case. We conclude that the problem of cylindrically anisotropic tubes under extension, torsion, shearing and pressuring is stable by homogenization and we define the effective tensor of the material elastic coefficients. Some numerical examples confirm the theoretical results.

1. Introduction

Bonding strength of layered composites, residual and thermal stresses in bonded dissimilar materials and wear resistant layers in machine, engine and structural components have attracted the attention of many researchers in recent years. The problems related to discontinuous material properties of multilayered materials made of very fine layers or the micro-macromechanical analysis of two-dimensional composites, such as the oscillatory behavior of deformation quantities or stresses resulting from material property mismatch, and the anisotropy induced by the homogenization procedure, are of great technological importance (see, for instance, Drago and Pindera, 2007). Functionally graded interlayers are used to reduce the above effects (Batra and Love, 2006; Cavalcante et al., 2007). The effect of non-homogeneity on the response of a cylindrical tube was first studied by Geymonat et al. (1987a,b) and recently investigated by Horgan and Chan (1999a,b), Chen et al. (2000), Tarn and Wang (2001), Tarn (2002b,a), Ruhi et al. (2005) and Boussaa (2006). For large differences of parameters of multi-component periodic materials made of very fine layers, additional interlayers are not the best solution and therefore we need the analysis of the behavior of the non-homogeneous material as well as the related behavior of the homogenized material obtained by assuming that the typical size of the layers ε tends to zero. As recently discussed in the context of exact elasticity solutions to the contact and crack problems in multilayered media with large moduli contrasts in Chen et al. (2005) and Pindera and Chen (2007), homogenization does break down in the presence of fine microstructures when the stress gradients are large. In Chen et al. (2005) the effects of microstructural refinement and homogenization on the contact pressure and sub-surface stresses for the flat punch contact problem on periodically laminated multilayers were studied and the concept of partial homogenization was introduced leading to stress exhibiting very high stress gradients at the top layers.

The intent of this paper is to present a self-contained treatment of some homogenization problems of a hollow circular cylinder composed of an elastic multilayered material with properties exhibiting discontinuities in the radial direction.

* Corresponding author. Tel.: +30 2310995931; fax: +30 2310995679.
E-mail address: charalam@civil.auth.gr (N. Charalambakis).

0020-7683/$ - see front matter © 2008 Elsevier Ltd. All rights reserved.
doi:10.1016/j.ijsolstr.2008.05.015

Mathematical homogenization consists in setting the problem as a sequence of equations describing the non-homogeneous material when the typical size ε of the heterogeneities becomes smaller and smaller. To quote only a few works of the generic research on this field, we mention Tartar (1977), Murat (1977), Bensoussan et al. (1978), Sanchez-Palencia (1978) and Suquet (1982).

We first show in Sections 2 and 3, with the help of two simple examples, that homogenization of isotropic materials causes anisotropy. In the first example, we present the homogenization of the equations describing the torsion of a periodic isotropic cylinder. The second example in Section 3 is the homogenization of the axisymmetric pressurized isotropic hollow cylinder subjected to prescribed uniform pressures at the inner and outer surfaces. Numerical results in Sections 2 and 3 confirm the theoretical findings.

The above results indicate that the isotropic material is not stable by homogenization. So in Section 4 we treat the torsion of a layered tube made of anisotropic materials.

Finally, in Section 5 we study the homogenization of the equations describing the general axisymmetric state as formulated by Tarn and Wang (2001). In this section, we find all anisotropic effective coefficients in terms of coefficients of the heterogeneous tube. The problem of cylindrically anisotropic materials turns to be stable by homogenization, in the sense that no other anisotropy is added as in the isotropic case. The homogenization results are illustrated by a numerical example at the end of this section. It is worth noticing that all stress field discontinuities correspond to those stress components which are not traction generated components.

In the sequel, we refer to the tube described in Fig. 1. Using polar coordinates r, θ, z, the radial, angular and longitudinal displacements are, respectively, u_r, u_θ, u_z and the strains are given by

$$\epsilon_{rr}=\frac{\partial u_r}{\partial r},\quad \epsilon_{\theta\theta}=\frac{1}{r}\left(\frac{\partial u_\theta}{\partial\theta}+u_r\right),\quad \epsilon_{zz}=\frac{\partial u_z}{\partial z},\quad \epsilon_{z\theta}=\frac{1}{2}\left(\frac{\partial u_\theta}{\partial z}+\frac{1}{r}\frac{\partial u_z}{\partial\theta}\right),\quad \epsilon_{rz}=\frac{1}{2}\left(\frac{\partial u_z}{\partial r}+\frac{\partial u_r}{\partial z}\right),$$
$$\epsilon_{r\theta}=\frac{1}{2}\left(\frac{1}{r}\frac{\partial u_r}{\partial\theta}+\frac{\partial u_\theta}{\partial r}-\frac{u_\theta}{r}\right). \tag{1}$$

The stress–displacement elastic constitutive laws are given by

$$\begin{bmatrix}\sigma_{rr}\\ \sigma_{\theta\theta}\\ \sigma_{zz}\\ \sigma_{z\theta}\\ \sigma_{rz}\\ \sigma_{r\theta}\end{bmatrix}=\begin{bmatrix}C_{11}&C_{12}&C_{13}&C_{14}&0&0\\ C_{12}&C_{22}&C_{23}&C_{24}&0&0\\ C_{13}&C_{23}&C_{33}&C_{34}&0&0\\ C_{14}&C_{24}&C_{34}&C_{44}&0&0\\ 0&0&0&0&C_{55}&C_{56}\\ 0&0&0&0&C_{56}&C_{66}\end{bmatrix}\begin{bmatrix}\frac{\partial u_r}{\partial r}\\ \frac{1}{r}\left(\frac{\partial u_\theta}{\partial\theta}+u_r\right)\\ \frac{\partial u_z}{\partial z}\\ \frac{\partial u_\theta}{\partial z}+\frac{1}{r}\frac{\partial u_z}{\partial\theta}\\ \frac{\partial u_z}{\partial r}+\frac{\partial u_r}{\partial z}\\ \frac{1}{r}\frac{\partial u_r}{\partial\theta}+\frac{\partial u_\theta}{\partial r}-\frac{u_\theta}{r}\end{bmatrix}, \tag{2}$$

and the equations of equilibrium read

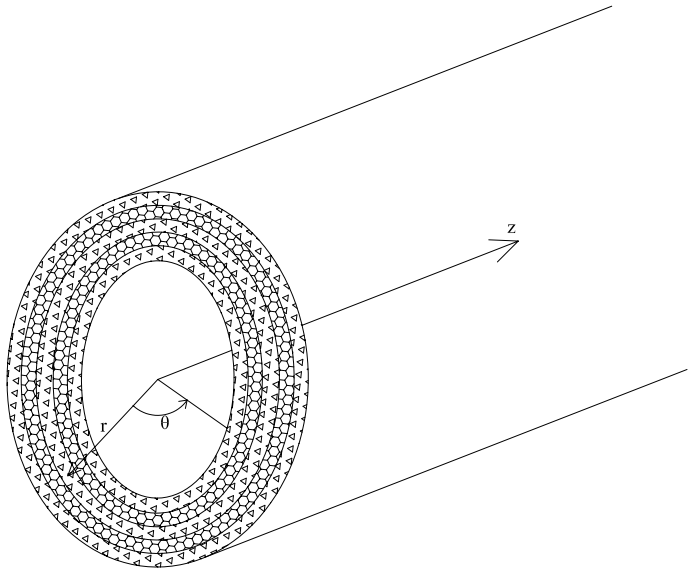

Fig. 1. Polar coordinates in the multilayered hollow cylinder.

$$\frac{\partial \sigma_{rr}}{\partial r}+\frac{1}{r}\frac{\partial \sigma_{r\theta}}{\partial \theta}+\frac{\sigma_{rr}-\sigma_{\theta\theta}}{r}+\frac{\partial \sigma_{rz}}{\partial z}=0, \tag{3}$$

$$\frac{\partial \sigma_{r\theta}}{\partial r}+\frac{1}{r}\frac{\partial \sigma_{\theta\theta}}{\partial \theta}+2\frac{\sigma_{r\theta}}{r}+\frac{\partial \sigma_{z\theta}}{\partial z}=0, \tag{4}$$

$$\frac{\partial \sigma_{zr}}{\partial r}+\frac{1}{r}\frac{\partial \sigma_{z\theta}}{\partial \theta}+\frac{\partial \sigma_{zz}}{\partial z}+\frac{\sigma_{zr}}{r}=0. \tag{5}$$

This system of partial differential equations, supplemented by suitable boundary conditions, describes the elastic problem of hollow cylinder.

2. Anisotropy induced by homogenization. First "generic problem: torsion

We first consider the multilayered tube of Fig. 1 subjected to prescribed displacement at the inner surface and transverse shear stresses at the inner surface and the two extremities. The tube is made of numerous isotropic layers of small thickness ε of very dissimilar materials. The parameter of heterogeneity ε enters to all functions of the system (1)–(5) of the previous section. We assume

$$u_r^\varepsilon = u_z^\varepsilon = 0, \quad u_\theta^\varepsilon = v^\varepsilon(r,z). \tag{6}$$

The transverse shear stress at a distance r and the shear stress acting on the cross section, respectively, are calculated from (2)

$$\sigma_{r\theta}^\varepsilon = \mu^\varepsilon\left(\frac{\partial v^\varepsilon}{\partial r}-\frac{v^\varepsilon}{r}\right), \quad \sigma_{z\theta}^\varepsilon = \mu^\varepsilon\frac{\partial v^\varepsilon}{\partial z}, \tag{7}$$

where

$$C_{44}^\varepsilon = C_{66}^\varepsilon = \mu^\varepsilon = \frac{E^\varepsilon}{2(1+\nu^\varepsilon)}. \tag{8}$$

The only equilibrium equation for $a \leqslant r \leqslant b$ is obtained from (4)

$$\frac{\partial \sigma_{r\theta}^\varepsilon}{\partial r}+2\frac{\sigma_{r\theta}^\varepsilon}{r}+\frac{\partial \sigma_{z\theta}^\varepsilon}{\partial z}=0, \tag{9}$$

(3) and (5) being satisfied as identities. The torsion is caused by prescribed displacement and prescribed transverse shear stress at the inner surface,

$$v^\varepsilon(a,z) = v_a(z), \quad \sigma_{r\theta}^\varepsilon(a,z) = \sigma_1(z), \tag{10}$$

and at the two ends of the tube

$$\sigma_{r\theta}^\varepsilon(r,0) = \sigma_2(r), \quad \sigma_{r\theta}^\varepsilon(r,\ell) = \sigma_3(r). \tag{11}$$

Assume that μ^ε varies with respect to r only

$$\mu^\varepsilon = \mu^\varepsilon(r), \quad 0 < \mu_1 \leqslant \mu^\varepsilon \leqslant \mu_2. \tag{12}$$

From (8) and (7)

$$\frac{\partial}{\partial r}\left(\mu^\varepsilon\left(\frac{\partial v^\varepsilon}{\partial r}-\frac{v^\varepsilon}{r}\right)\right)+\frac{2}{r}\mu^\varepsilon\left(\frac{\partial v^\varepsilon}{\partial r}-\frac{v^\varepsilon}{r}\right)+\frac{\partial}{\partial z}\left(\mu^\varepsilon\frac{\partial v^\varepsilon}{\partial z}\right)=0. \tag{13}$$

We assume that v^ε is oscillating only with respect to r. Moreover, we assume

$$v^\varepsilon(r,z) = X^\varepsilon(r)Z(z). \tag{14}$$

Then, (13) gives

$$Z(z)\frac{\mathrm{d}}{\mathrm{d}r}\left(\mu^\varepsilon(r)\left(\frac{\mathrm{d}X^\varepsilon(r)}{\mathrm{d}r}-\frac{1}{r}X^\varepsilon(r)\right)\right)+\frac{2}{r}\mu^\varepsilon(r)Z(z)\left(\frac{\mathrm{d}X^\varepsilon(r)}{\mathrm{d}r}-\frac{1}{r}X^\varepsilon(r)\right)+\mu^\varepsilon(r)X^\varepsilon(r)\frac{\mathrm{d}^2Z(z)}{\mathrm{d}z^2}=0. \tag{15}$$

This equation is equivalent to the following system of ordinary differential equations for $X^\varepsilon(r)$, $\omega^\varepsilon(r)$ and $Z(z)$,

$$Z(z)\left[\frac{\mathrm{d}\omega^\varepsilon(r)}{\mathrm{d}r}+\frac{2}{r}\omega^\varepsilon(r)\right]+\mu^\varepsilon(r)X^\varepsilon(r)\frac{\mathrm{d}^2Z(z)}{\mathrm{d}z^2}=0, \tag{16}$$

$$\mu^\varepsilon(r)\left(\frac{\mathrm{d}X^\varepsilon(r)}{\mathrm{d}r}-\frac{1}{r}X^\varepsilon(r)\right)=\omega^\varepsilon(r), \tag{17}$$

$$\frac{\mathrm{d}^2Z(z)}{\mathrm{d}z^2}=k^2Z, \tag{18}$$

where k an arbitrary constant, submitted to the boundary conditions

$$Z(0) = Z_1, \quad Z(\ell) = Z_2, \tag{19}$$

$$\omega(a) = \omega_a > 0, \quad X(a) = X_a > 0. \tag{20}$$

From (18) and (19)

$$Z(z) = \frac{Z_2 - Z_1 e^{-k\ell}}{e^{k\ell} - e^{-k\ell}} e^{kz} + \frac{Z_1 e^{k\ell} - Z_2}{e^{k\ell} - e^{-k\ell}} e^{-kz}. \tag{21}$$

For $Z(z) \neq 0$, (16), (17) are equivalent to the following system of ordinary differential equations with unknowns $\omega^\varepsilon(r)$ and $X^\varepsilon(r)$

$$\frac{\mathrm{d}\omega^\varepsilon(r)}{\mathrm{d}r} + \frac{2}{r}\omega^\varepsilon(r) + k^2 \mu^\varepsilon(r) X^\varepsilon(r) = 0, \tag{22}$$

$$\mu^\varepsilon(r)\frac{\mathrm{d}X^\varepsilon(r)}{\mathrm{d}r} - \frac{1}{r}\mu^\varepsilon(r) X^\varepsilon(r) = \omega^\varepsilon(r), \tag{23}$$

under the boundary conditions (20). We conclude (see Appendix A) that X^ε and $\omega^\varepsilon(r)$ are continuous. Therefore there exist a subsequence $X^{\varepsilon'}$, still denoted by X^ε, and X^h, and a subsequence $\omega^{\varepsilon'}$, still denoted by ω^ε, and a ω^h such that

$$X^\varepsilon \to X^h \text{ in } C(a,b), \tag{24}$$

$$\omega^\varepsilon \to \omega^h \text{ in } C(a,b), \tag{25}$$

and we can pass to the limit in (22), (23). In the sequel, we prove that X^h and ω^h are given, respectively, by (31) and (32), therefore X^h and ω^h are unique, so there is no need to extract subsequences and the whole subsequence converge. From (22) we obtain the homogenized equation satisfied by ω^h in terms of X^h,

$$\frac{\mathrm{d}\omega^h(r)}{\mathrm{d}r} + \frac{2}{r}\omega^h(r) + k^2 \mu^h(r) X^h(r) = 0. \tag{26}$$

We now assume that μ^ε is periodic. Then μ^ε converges weakly to its mean value,

$$\mu^h = \langle \mu^\varepsilon \rangle. \tag{27}$$

On the other hand, from (23) we obtain that X^h is the solution of

$$\frac{\mathrm{d}X^h(r)}{\mathrm{d}r} - \frac{1}{r}X^h(r) = \left\langle \frac{1}{\mu^\varepsilon} \right\rangle \omega^h(r). \tag{28}$$

From (28)

$$\omega^h(r) = \frac{1}{\left\langle \frac{1}{\mu^\varepsilon} \right\rangle}\frac{\mathrm{d}X^h(r)}{\mathrm{d}r} - \frac{1}{r}\frac{1}{\left\langle \frac{1}{\mu^\varepsilon} \right\rangle} X^h(r), \tag{29}$$

and substituting in (26) we obtain the homogenized differential equation for X^h,

$$\frac{\mathrm{d}^2 X^h(r)}{\mathrm{d}r^2} + \frac{1}{r}\frac{\mathrm{d}X^h(r)}{\mathrm{d}r} + \left(k^2 \langle \mu^\varepsilon \rangle \left\langle \frac{1}{\mu^\varepsilon} \right\rangle - \frac{1}{r^2} \right) X^h(r) = 0. \tag{30}$$

The solution of the homogenized Eq. (30) is of the form

$$X^h = A_1 J_1\left(\sqrt{k^2 \langle \mu^\varepsilon \rangle \left\langle \frac{1}{\mu^\varepsilon} \right\rangle} r \right) + B_1 Y_1\left(\sqrt{k^2 \langle \mu^\varepsilon \rangle \left\langle \frac{1}{\mu^\varepsilon} \right\rangle} r \right), \tag{31}$$

where J_1, Y_1 Bessel functions of first and second kind, respectively, and A_1, B_1 arbitrary constants. Substituting (31) in (28) we get

$$\omega^h = -\sqrt{k^2 \frac{\langle \mu^\varepsilon \rangle}{\langle 1/\mu^\varepsilon \rangle}} \left[A_1 J_2\left(\sqrt{k^2 \langle \mu^\varepsilon \rangle \left\langle \frac{1}{\mu^\varepsilon} \right\rangle} r \right) + B_1 Y_2\left(\sqrt{k^2 \langle \mu^\varepsilon \rangle \left\langle \frac{1}{\mu^\varepsilon} \right\rangle} r \right) \right], \tag{32}$$

By putting the boundary condition (20) in (31) and (32) we compute the constants A_1, B_1,

$$A_1 = \frac{X_a Y_2(\tilde{a}) + \omega_a Y_1(\tilde{a}) \sqrt{\frac{\langle 1/\mu^\varepsilon \rangle}{k^2 \langle \mu^\varepsilon \rangle}}}{J_1(\tilde{a}) Y_2(\tilde{a}) - Y_1(\tilde{a}) J_2(\tilde{a})}, \quad B_1 = \frac{X_a J_2(\tilde{a}) + \omega_a J_1(\tilde{a}) \sqrt{\frac{\langle 1/\mu^\varepsilon \rangle}{k^2 \langle \mu^\varepsilon \rangle}}}{Y_1(\tilde{a}) J_2(\tilde{a}) - J_1(\tilde{a}) Y_2(\tilde{a})}, \tag{33}$$

where

$$\tilde{a} = \sqrt{k^2 \langle \mu^\varepsilon \rangle \left\langle \frac{1}{\mu^\varepsilon} \right\rangle} a. \tag{34}$$

Then, the displacement and the stresses of the homogenized material are given by the expressions

$$v^h = \int_0^\infty X^h(r,k)Z(z,k)\mathrm{d}k, \quad \sigma^h_{r\theta} = \int_0^\infty \omega^h(r,k)Z(z,k)\mathrm{d}k, \tag{35}$$

$$\sigma^h_{z\theta} = \int_0^\infty \langle\mu^\varepsilon\rangle X^h(r,k)\frac{\mathrm{d}Z}{\mathrm{d}z}(z,k)\mathrm{d}k. \tag{36}$$

where $Z(z,k)$ is given by (21) and $X^h(r,k)$, $\omega^h(r,k)$ are given by (31), (32), respectively.

We can easily verify that the results show a homogenization-induced anisotropy, since for the isotropic non-homogeneous material the stresses are calculated in terms of strains with the help of the same elastic coefficient μ^ε,

$$\sigma^\varepsilon_{r\theta} = 2\mu^\varepsilon\epsilon^\varepsilon_{r\theta},$$
$$\sigma^\varepsilon_{z\theta} = 2\mu^\varepsilon\epsilon^\varepsilon_{z\theta},$$

while for the homogenized medium

$$\sigma^\varepsilon_{r\theta} \to \sigma^h_{r\theta} = 2\frac{1}{\left\langle\frac{1}{\mu^\varepsilon}\right\rangle}\epsilon^h_{r\theta},$$
$$\sigma^\varepsilon_{z\theta} \rightharpoonup \sigma^h_{z\theta} = 2\langle\mu^\varepsilon\rangle\epsilon^h_{z\theta}.$$

There are two planes of cylindrical orthotropy: on the cross section the effective coefficient is equal to the mean value of the non-homogeneous coefficients, while in all planes parallel to the axis z the effective coefficient is equal to the inverse of the mean value of the inverse non-homogeneous coefficients.

2.1. Numerical example: periodic hollow cylinder under torsion

In this first example we consider a hollow cylinder consisting of 20 multiple periodic layers, of two isotropic materials. The shear modulus of these materials varies, as in Fig. 2. We choose the sigmoid function (Seto and Nishimura, 2004), whose form can be found in Chatzigeorgiou et al. (2007), in order to approximate the discontinuity between the layers with continuous function. The radii of inner and outer surfaces are $a = 0.1$ m and $b = 0.2$ m, respectively. The length of cylinder is $\ell = 2$ m. We assume the boundary conditions

$$X_a = 1, \quad \omega_a = 10,000, \quad Z_1 = 0.002\mathrm{e}^{-2k\ell}, \quad Z_2 = 0.002\mathrm{e}^{-k\ell}.$$

The system of Eqs. (22) and (23) is treated as an initial value problem and it is solved with the fourth order Runge–Kutta Method. For the homogenized material, the explicit form of equations is inserted in software *Mathematica*. Fig. 3a presents the angular displacement of the cylinder as a function of radius at $z = \ell$. We observe that the displacement varies linearly with the radius. The transverse shear stress $\sigma_{r\theta}$ takes negative values, as it can be seen in Fig. 3b. For the homogenized material, both the angular displacement u_θ and $\sigma_{r\theta}$ practically coincide with these of the non-homogeneous material. The distribution of in-plane shear stress $\sigma_{z\theta}$ is oscillatory and is given in Fig. 3c. In the same figure we also present the stress $\sigma_{z\theta}$ of the homogenized material. The "jumps" of $\sigma_{z\theta}$ increase following the increase of $\sigma_{z\theta}$ along the z-axis. Close to inner and outer

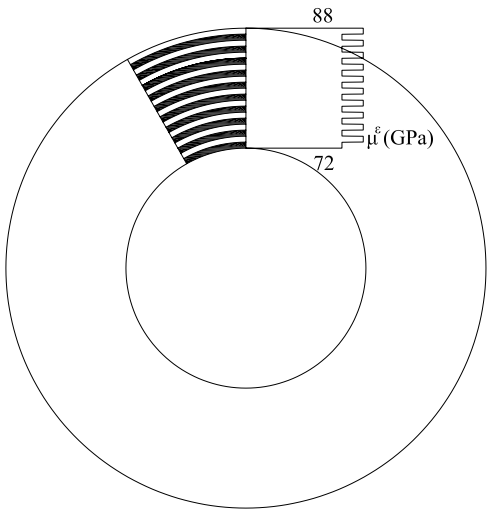

Fig. 2. Radial variation of shear modulus μ^ε in the multilayered isotropic hollow cylinder.

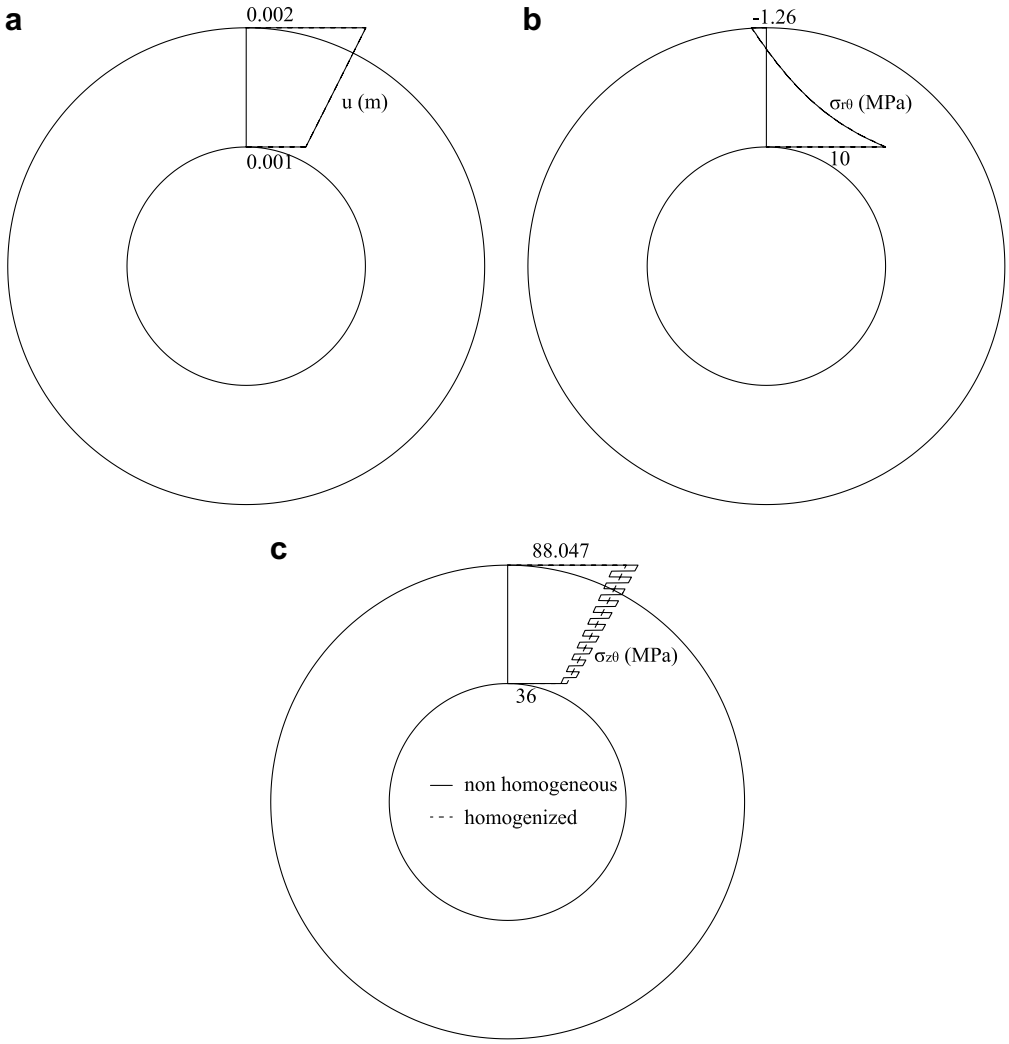

Fig. 3. (a) Angular displacement (non-homogeneous and homogenized values practically coincide), (b) transversal (non-homogeneous and homogenized values with 1% difference) and (c) in-plane shear stresses of hollow cylinder at $z = 2$ m.

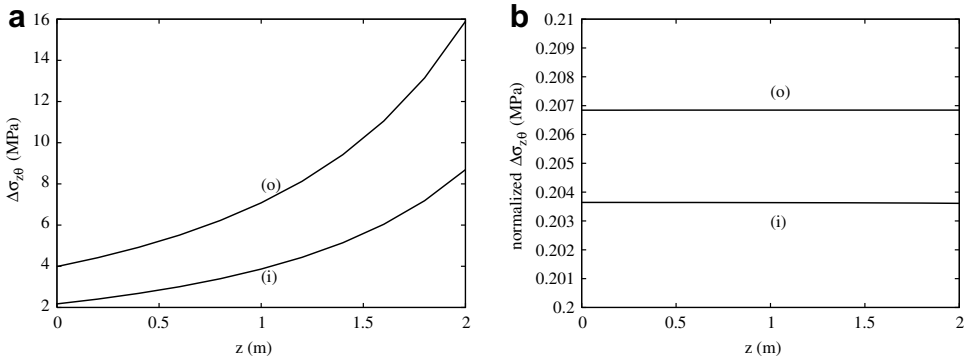

Fig. 4. Variation of the "jump" of the in-plane shear stress $\sigma_{z\theta}$ and the corresponding normalized at the inner (i) and the outer (o) surfaces with respect to z.

surfaces the "jumps" vary with z according to Fig. 4a. On the contrary, the normalized "jumps" ("jumps" in the in-plane shear stress divided by the corresponding homogenized stress) remain constant (Fig. 4b). In Fig. 5 we see the angular displacement and the stresses at the inner and outer surfaces.

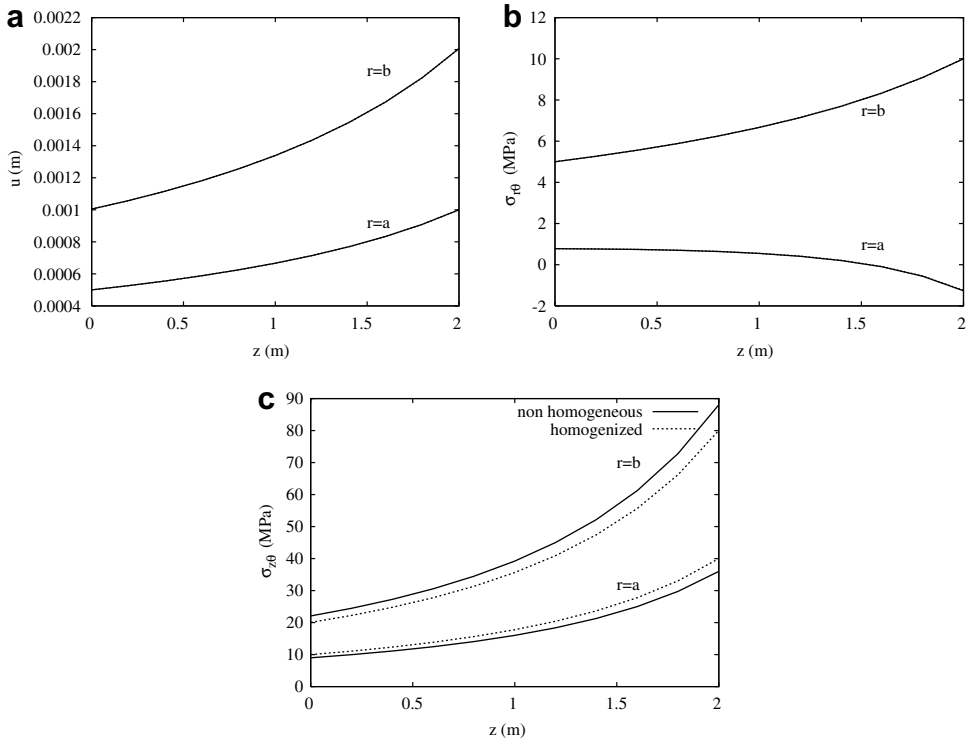

Fig. 5. Variation with z of (a) angular displacement u, (b) transverse shear stress $\sigma_{r\theta}$ and (c) in-plane shear stress $\sigma_{z\theta}$ at the inner and outer surfaces.

2.2. Numerical example: graded hollow cylinder under torsion

We now examine the case of a hollow cylinder consisting of 20 multiple layers, with discontinuously graded structure. For comparison reasons, we also examine a hollow cylinder with continuously graded structure. The variation of shear modulus for these cylinders is shown in Fig. 6a. We choose again the sigmoid function, in order to approximate the discontinuity between the layers with continuous function. The geometrical characteristics and the boundary conditions are exactly the same with these of the previous example. As we observe in Figs. 6b and 6c, the stress $\sigma_{z\theta}$ progressively increases from 30 to 100 MPa. The behavior of the continuously graded cylinder is in a good agreement with this of the discontinuously graded cylinder.

3. Anisotropy induced by homogenization. Second "generic problem: pressurized hollow cylinder

In this section, we consider the axisymmetric problem of a hollow circular cylinder subjected to uniform pressure on the inner and outer surfaces. Let a and b denote again the inner and outer radii, and p_i and p_0 the internal and external pressures, respectively. We are concerned only with axisymmetric deformations, so that the only displacement component is $u_r^\varepsilon(r) = u^\varepsilon(r)$. It is assumed that the body is composed of very fine layers of thickness ε of very dissimilar elastic isotropic materials.

Under plane stress, the non-zero normal stresses σ_{rr}^ε and $\sigma_{\theta\theta}^\varepsilon$ are given in terms of the radial displacement by

$$\sigma_{rr}^\varepsilon(r) = C_{11}^\varepsilon(r)\frac{\mathrm{d}u^\varepsilon(r)}{\mathrm{d}r} + C_{12}^\varepsilon(r)\frac{u^\varepsilon(r)}{r} = \frac{E^\varepsilon(r)}{1-(\nu^\varepsilon(r))^2}\left(\frac{\mathrm{d}u^\varepsilon(r)}{\mathrm{d}r} + \nu^\varepsilon(r)\frac{u^\varepsilon(r)}{r}\right), \tag{37}$$

$$\sigma_{\theta\theta}^\varepsilon(r) = C_{22}^\varepsilon\frac{u^\varepsilon(r)}{r} + C_{12}^\varepsilon(r)\frac{\mathrm{d}u^\varepsilon(r)}{\mathrm{d}r} = \frac{E^\varepsilon(r)}{1-(\nu^\varepsilon(r))^2}\left(\frac{u^\varepsilon(r)}{r} + \nu^\varepsilon(r)\frac{\mathrm{d}u^\varepsilon(r)}{\mathrm{d}r}\right). \tag{38}$$

For the hollow cylinder under plane strain, the analogs of the above constitutive equations are obtained on formally replacing E^ϵ and ν^ϵ, respectively, by M^ε and N^ε, where

$$M^\varepsilon = \frac{E^\varepsilon(r)}{1-(\nu^\varepsilon(r))^2}, \quad N^\varepsilon = \frac{\nu^\varepsilon(r)}{1-\nu^\varepsilon(r)}. \tag{39}$$

In this case, the normal stress parallel to the axis z is given by

$$\sigma_{zz}^\varepsilon(r) = \nu^\varepsilon(r)(\sigma_{rr}^\varepsilon(r) + \sigma_{\theta\theta}^\varepsilon(r)). \tag{40}$$

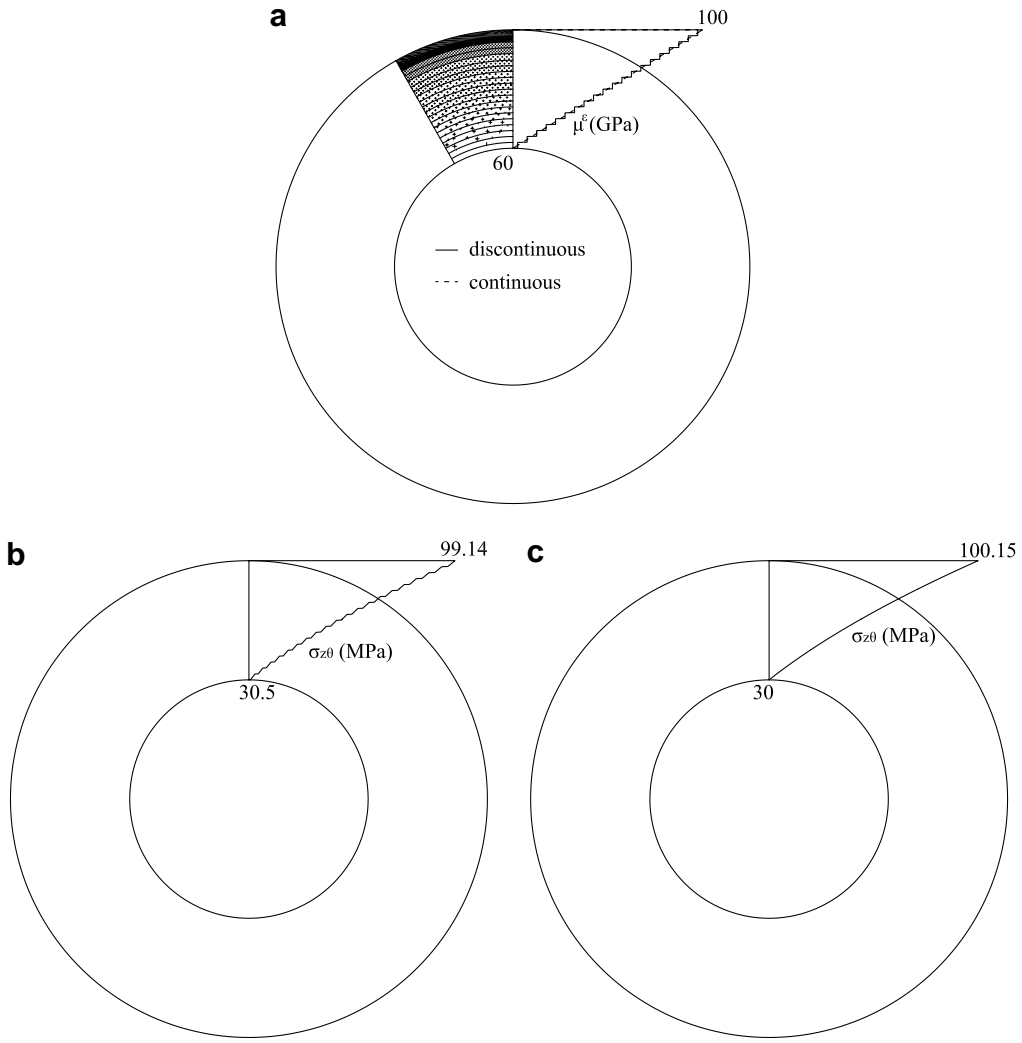

Fig. 6. (a) Radial variation of shear modulus in the discontinuously graded hollow cylinder. (b) In-plane shear stress $\sigma_{z\theta}$ at $z = 2$ m for discontinuously graded structure and (c) in-plane shear stress $\sigma_{z\theta}$ at $z = 2$ m for continuously graded structure of the hollow cylinder.

E^{ε}, v^{ε} are Young modulus and Poisson's ratio, respectively. Since the spatial variation in Poisson's ratio is of much less practical importance than that in the Young's modulus, we assume that $v^{\varepsilon}(r)(N^{\varepsilon}(r))$ varies only in $E^{\varepsilon}(r)/(1-(v^{\varepsilon}(r))^2)$ $(M^{\varepsilon}(r)/(1-(N^{\varepsilon}(r))^2))$ in (37), (38), (40). Putting

$$\begin{aligned} A^{\varepsilon}(r) &= \frac{E^{\varepsilon}(r)}{1-(v^{\varepsilon}(r))^2} \ \text{(plane stress)}, \\ A^{\varepsilon}(r) &= \frac{M^{\varepsilon}(r)}{1-(N^{\varepsilon}(r))^2} \ \text{(plane strain)}, \end{aligned} \tag{41}$$

in (37), (38) yields

$$\sigma^{\varepsilon}_{rr}(r) = A^{\varepsilon}(r)\left(\frac{\mathrm{d}u^{\varepsilon}(r)}{\mathrm{d}r} + N\frac{u^{\varepsilon}(r)}{r}\right), \tag{42}$$

$$\sigma^{\varepsilon}_{\theta\theta}(r) = A^{\varepsilon}(r)\left(\frac{u^{\varepsilon}(r)}{r} + N\frac{\mathrm{d}u^{\varepsilon}(r)}{\mathrm{d}r}\right), \tag{43}$$

and from the equations of equilibrium (see (3)),

$$\frac{\mathrm{d}\sigma^{\varepsilon}_{rr}}{\mathrm{d}r} + \frac{\sigma^{\varepsilon}_{rr} - \sigma^{\varepsilon}_{\theta\theta}}{r} = 0, \tag{44}$$

or

$$\frac{\mathrm{d}}{\mathrm{d}r}\left[A^{\varepsilon}(r)\left(\frac{\mathrm{d}u^{\varepsilon}(r)}{\mathrm{d}r}+N\frac{u^{\varepsilon}(r)}{r}\right)\right]+(1-N)\frac{A^{\varepsilon}(r)}{r}\left(\frac{\mathrm{d}u^{\varepsilon}(r)}{\mathrm{d}r}-\frac{u^{\varepsilon}(r)}{r}\right)=0, \tag{45}$$

subjected to boundary conditions

$$\sigma_{rr}(a)=-p_i,\sigma_{rr}(b)=-p_o. \tag{46}$$

We assume that A^{ε} is a, non-necessarily smooth, function bounded from above and from below by strictly positive constants. In Section 5, we prove that, for the general anisotropic case, $|u^{\varepsilon}|$ and $|\frac{\mathrm{d}u^{\varepsilon}}{\mathrm{d}r}|$ are bounded independently of ε, so u^{ε} is continuous and there exists a subsequence $u^{\varepsilon'}$, still denoted by u^{ε}, and a u^h such that

$$u^{\varepsilon}\to u^h \text{ in } C(a,b). \tag{47}$$

In view of (37) and (44) and of the bounds of $|\frac{\mathrm{d}u^{\varepsilon}}{\mathrm{d}r}|$ we have that $|\sigma^{\varepsilon}_{rr}|$ and $|\frac{\mathrm{d}\sigma^{\varepsilon}_{rr}}{\mathrm{d}r}|$ are bounded independently of ε, so $\sigma^{\varepsilon}_{rr}$ is continuous and there exists a subsequence $\sigma^{\varepsilon'}$, still denoted by $\sigma^{\varepsilon}_{rr}$, and a σ^h_{rr} such that

$$\sigma^{\varepsilon}_{rr}\to\sigma^h_{rr} \text{ in } C(a,b). \tag{48}$$

Eqs. (42) and (43) give

$$\sigma^{\varepsilon}_{\theta\theta}(r)=N\sigma^{\varepsilon}_{rr}(r)+\frac{1-N^2}{r}A^{\varepsilon}(r)u^{\varepsilon}(r), \tag{49}$$

from which we get that $\sigma^{\varepsilon}_{\theta\theta}$ is bounded in L^{∞} and there exist a subsequence, still denoted by $\sigma^{\varepsilon}_{\theta\theta}$, and a $\sigma^h_{\theta\theta}$ such that

$$\sigma^{\varepsilon}_{\theta\theta}\rightharpoonup\sigma^h_{\theta\theta} \text{ in } L^{\infty}(a,b) \text{ weak star}. \tag{50}$$

So, from Eq. (40) we deduce that

$$\sigma^{\varepsilon}_{zz}\rightharpoonup\sigma^h_{zz} \text{ in } L^{\infty}(a,b) \text{ weak star}. \tag{51}$$

We note that in case of homogeneous materials, equation (45) accompanied by the boundary conditions (46) has the analytical solution

$$u(r)=\frac{cr}{A(1+N)}+\frac{d/r}{A(1-N)}, \tag{52}$$

where

$$c=-\frac{p_ob^2-p_ia^2}{b^2-a^2},\quad d=-\frac{p_o-p_i}{b^2-a^2}a^2b^2. \tag{53}$$

Moreover,

$$\sigma_{rr}(r)=c-\frac{d}{r^2},\quad \sigma_{\theta\theta}(r)=c+\frac{d}{r^2},\quad \sigma_{zz}(r)=2\nu c. \tag{54}$$

In conclusion, the system of equations that describe the non-homogeneous problem is

$$\frac{\mathrm{d}\sigma^{\varepsilon}_{rr}}{\mathrm{d}r}=\frac{1-N^2}{r^2}A^{\varepsilon}u^{\varepsilon}-\frac{1-N}{r}\sigma^{\varepsilon}_{rr}, \tag{55}$$

$$\frac{\mathrm{d}u^{\varepsilon}}{\mathrm{d}r}=\frac{1}{A^{\varepsilon}}\sigma^{\varepsilon}_{rr}-\frac{N}{r}u^{\varepsilon}, \tag{56}$$

$$\sigma^{\varepsilon}_{\theta\theta}=N\sigma^{\varepsilon}_{rr}+\frac{1-N^2}{r}A^{\varepsilon}u^{\varepsilon}, \tag{57}$$

$$\sigma^{\varepsilon}_{zz}=\nu(\sigma^{\varepsilon}_{rr}+\sigma^{\varepsilon}_{\theta\theta}). \tag{58}$$

From (47) and (48), we easily prove that the system of equations that describe the homogenized material is

$$\frac{\mathrm{d}\sigma^h_{rr}}{\mathrm{d}r}=\frac{1-N^2}{r^2}\langle A^{\varepsilon}\rangle u^h-\frac{1-N}{r}\sigma^h_{rr}, \tag{59}$$

$$\frac{\mathrm{d}u^h}{\mathrm{d}r}=\left\langle\frac{1}{A^{\varepsilon}}\right\rangle\sigma^h_{rr}-\frac{N}{r}u^h, \tag{60}$$

$$\sigma^h_{\theta\theta}=N\sigma^h_{rr}+\frac{1-N^2}{r}\langle A^{\varepsilon}\rangle u^h, \tag{61}$$

$$\sigma^h_{zz}=\nu(\sigma^h_{rr}+\sigma^h_{\theta\theta}). \tag{62}$$

From (60) we obtain the expression for the homogenized radial normal stress

$$\sigma^h_{rr}=\frac{1}{\left\langle\frac{1}{A^{\varepsilon}}\right\rangle}\frac{\mathrm{d}u^h}{\mathrm{d}r}+\frac{1}{\left\langle\frac{1}{A^{\varepsilon}}\right\rangle}\frac{N}{r}u^h, \tag{63}$$

and from (61) and (63) the expression for the homogenized hoop stress

$$\sigma^h_{\theta\theta} = N\frac{1}{\left\langle\frac{1}{A^\varepsilon}\right\rangle}\frac{\mathrm{d}u^h}{\mathrm{d}r} + \left[(1-N^2)\langle A^\varepsilon\rangle + N^2\frac{1}{\left\langle\frac{1}{A^\varepsilon}\right\rangle}\right]\frac{1}{r}u^h, \tag{64}$$

Comparing (63), (64) with the non-homogeneous expressions (42), (43) leads to the homogenization-induced cylindrical orthotropy of the homogenized material mentioned in Section 1.

3.1. Numerical example: pressurized hollow cylinder

In this example, we again consider a hollow cylinder consisting of 200 thin periodic layers made of two isotropic materials. The mechanical parameter A^ε of these materials is shown in Fig. 7. The Poisson's ratio is 0.2. In the non-homogeneous numerical simulation, $A^\varepsilon(r)$ is approximated by a sigmoid function. The radial stress takes the values -30 MPa at the inner surface and -60 MPa at the outer surface. The inner and outer radii are again 0.1 m and 0.2 m, respectively. The system of Eqs. (55) and (56) is solved with the fourth order Runge–Kutta Method. The boundary conditions are satisfied with the help of the Shooting Method. The same procedure is followed for the solution of the system (59) and (60). Moreover, we compare the results of the above non-homogeneous case with the results obtained for two homogeneous isotropic materials: the material 1 with mechanical parameter $\langle A^\varepsilon\rangle$ and the material 2 with mechanical parameter $\frac{1}{\langle 1/A^\varepsilon\rangle}$. In Fig. 8a, we observe that the radial displacement of material 2 differs considerably from the radial displacements of the other three materials. The non-homogeneous and the homogenized material have the same behavior, while the material 1 shows a small deviation from these, with maximum difference 5%. Recalling that the stresses of the isotropic homogeneous materials are independent of the mechanical parameters ((54)), we show only one isotropic homogeneous material in Figs. 8b, 8c and 8d.

4. Torsion of anisotropic hollow cylinder

We first assume, as in Section 2, that the only non-zero displacement is $u_\theta = v(r,z)$. The equations of equilibrium (3)–(5) give with the above expressions of stress components three differential equations with respect to the displacement v^ε. It is obvious that the very simplistic assumptions on the displacement do not comply with the degree of anisotropy assumed for the material and that some elastic coefficients must be zero in order to reduce the number of equations of equilibrium. We can prove that necessarily

$$C^\varepsilon_{14}(r) = C^\varepsilon_{24}(r) = C^\varepsilon_{34}(r) = C^\varepsilon_{56}(r) = 0, \tag{65}$$

therefore the first and the third equation of equilibrium become identities and only the second one

$$\frac{\partial}{\partial r}\left[C^\varepsilon_{66}(r)\left(\frac{\partial v^\varepsilon}{\partial r} - \frac{1}{r}v^\varepsilon\right)\right] + \frac{2}{r}C^\varepsilon_{66}(r)\left(\frac{\partial v^\varepsilon}{\partial r} - \frac{1}{r}v^\varepsilon\right) + C^\varepsilon_{44}(r)\frac{\partial^2 v^\varepsilon}{\partial z^2} = 0 \tag{66}$$

can be used to provide information on the homogenization process. But this equation is of the same form with (13), except of the fact that it is anisotropic ($C^\varepsilon_{66} \neq C^\varepsilon_{44}$). The coefficients ($C^\varepsilon_{44}$ and C^ε_{66}) are bounded from above and from below by strictly positive constants and are allowed to exhibit discontinuities. Following the same lines as in Section 2, we can prove the strong convergence of the transverse shear stress and the weak convergence of the in-plane shear stress and find the effective elastic parameters for a tube of periodic structure, so that

$$\sigma^\varepsilon_{r\theta} \to \sigma^h_{r\theta} = \frac{1}{\left\langle\frac{1}{C^\varepsilon_{66}}\right\rangle}\epsilon^\varepsilon_{r\theta}, \sigma^\varepsilon_{z\theta} \rightharpoonup \sigma^h_{z\theta} = \langle C^\varepsilon_{44}\rangle\epsilon^\varepsilon_{z\theta}. \tag{67}$$

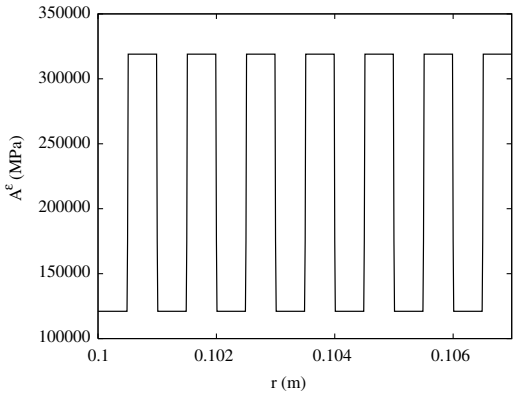

Fig. 7. Radial variation of elastic coefficient A^ε in the pressurized isotropic hollow cylinder.

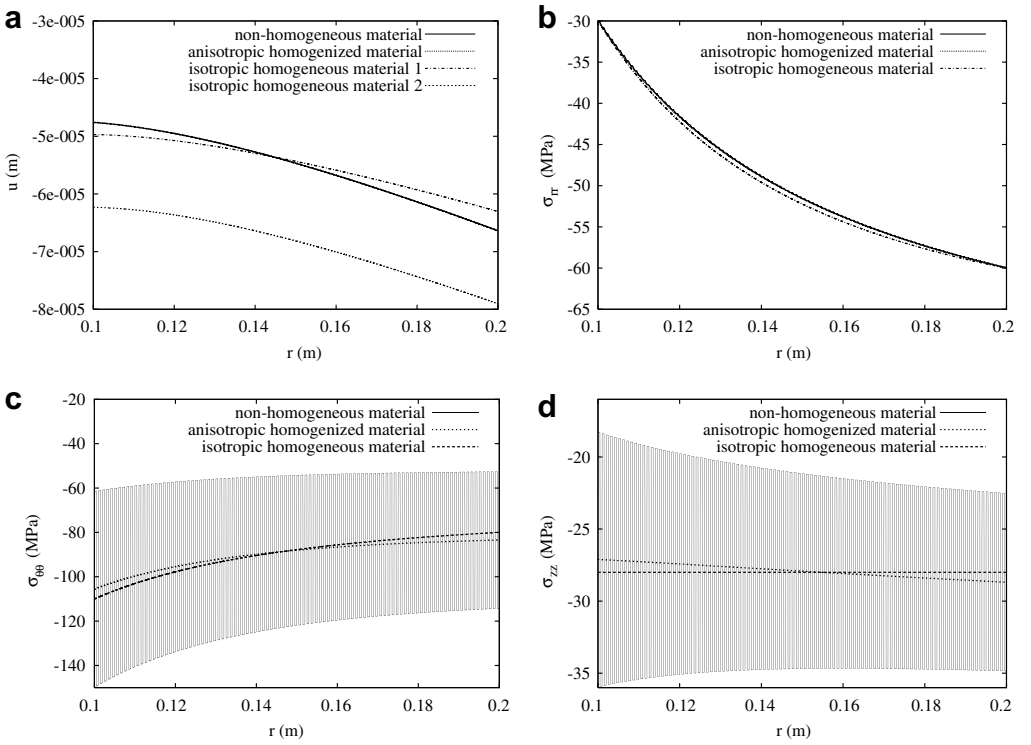

Fig. 8. Radial variation of (a) radial displacement (the curve of the non-homogeneous and the curve of the homogenized coincide with less than 0.2% error), (b) radial stress (the curve of the non-homogeneous and the curve of the homogenized coincide with less than 0.8% error), (c) hoop stress and (d) longitudinal stress in the pressurized isotropic hollow cylinder.

It turns out that the anisotropic formulation of a non-homogeneous material under torsion with $v_r^\varepsilon = v_z^\varepsilon = 0$ is stable by homogenization.

We now allow, in addition to the angular displacement v, the longitudinal displacement to be a function independent of z,

$$u_z = w(r,\theta) \tag{68}$$

and assume that the boundary conditions are now (10), (11) and

$$w(a,\theta) = w(\theta), \sigma_{rz}^\varepsilon(a,\theta) = \sigma_4(\theta), \sigma_{rz}^\varepsilon(r,0) = \sigma_5(r), \sigma_{rz}^\varepsilon\left(r,\frac{\pi}{2}\right) = \sigma_6(r). \tag{69}$$

Assuming again cylindrical orthotropy (65) yields the equations of equilibrium

$$\frac{\partial}{\partial z}\left(C_{55}^\varepsilon(r)\frac{\partial w^\varepsilon}{\partial r}\right) = 0, \tag{70}$$

$$\frac{\partial}{\partial r}\left(C_{55}^\varepsilon(r)\frac{\partial w^\varepsilon}{\partial r}\right) + \frac{1}{r}C_{55}^\varepsilon(r)\frac{\partial w^\varepsilon}{\partial r} + \frac{1}{r^2}C_{44}^\varepsilon(r)\frac{\partial^2 w^\varepsilon}{\partial \theta^2} = 0, \tag{71}$$

$$\frac{\partial}{\partial r}\left[C_{66}^\varepsilon(r)\left(\frac{\partial v^\varepsilon}{\partial r} - \frac{1}{r}v^\varepsilon\right)\right] + \frac{2}{r}C_{66}^\varepsilon(r)\left(\frac{\partial v^\varepsilon}{\partial r} - \frac{1}{r}v^\varepsilon\right) + C_{44}^\varepsilon(r)\frac{\partial^2 v^\varepsilon}{\partial z^2} = 0. \tag{72}$$

Eq. (70) is a identity, Eq. (72) is exactly of the same form with (66) (with z replaced by θ) and Eq. (71) can be treated in a similar way with (13) by putting

$$w(r,\theta) = X_1(r)\omega_1(\theta). \tag{73}$$

Following the same lines as in Section 2 and using the fact that (71) and (72) are uncoupled, we can prove that v^ε, w^ε converge strongly in $C(a,b)$. Then we can pass to the limit in (71) and (72) to find that the effective coefficients of a tube of periodic structure are

$$C_{44}^h = \langle C_{44}^\varepsilon \rangle, \quad C_{55}^h = \frac{1}{\left\langle \frac{1}{C_{55}^\varepsilon} \right\rangle}, \quad C_{66}^h = \frac{1}{\left\langle \frac{1}{C_{66}^\varepsilon} \right\rangle}. \tag{74}$$

5. Axisymmetric state of multilayered anisotropic hollow cylinder

In this section, we assume that the cylinder is made of numerous layers of anisotropic materials, following a periodic structure. Motivated by the axisymmetric case (axial force and torque at the ends, internal end external pressure, in-plane and anti-plane shears on the inner and outer surfaces), described by Tarn and Wang (2001), we assume that the stress and displacement fields are independent of the z-axis. Then the stress–displacement relation is given by the following system,

$$\begin{bmatrix} \sigma^{\varepsilon}_{rr} \\ \sigma^{\varepsilon}_{\theta\theta} \\ \sigma^{\varepsilon}_{zz} \\ \sigma^{\varepsilon}_{z\theta} \\ \sigma^{\varepsilon}_{rz} \\ \sigma^{\varepsilon}_{r\theta} \end{bmatrix} = \begin{bmatrix} C^{\varepsilon}_{11} & C^{\varepsilon}_{12} & 0 & 0 \\ C^{\varepsilon}_{12} & C^{\varepsilon}_{22} & 0 & 0 \\ C^{\varepsilon}_{13} & C^{\varepsilon}_{23} & 0 & 0 \\ C^{\varepsilon}_{14} & C^{\varepsilon}_{24} & 0 & 0 \\ 0 & 0 & C^{\varepsilon}_{55} & C^{\varepsilon}_{56} \\ 0 & 0 & C^{\varepsilon}_{56} & C^{\varepsilon}_{66} \end{bmatrix} \begin{bmatrix} \frac{\mathrm{d}u^{\varepsilon}_r}{\mathrm{d}r} \\ \frac{u^{\varepsilon}_r}{r} \\ \frac{\mathrm{d}u^{\varepsilon}_z}{\mathrm{d}r} \\ \frac{\mathrm{d}u^{\varepsilon}_\theta}{\mathrm{d}r} - \frac{u^{\varepsilon}_\theta}{r} \end{bmatrix}, \tag{75}$$

while the equilibrium equations give

$$\frac{\mathrm{d}\sigma^{\varepsilon}_{rr}}{\mathrm{d}r} + \frac{\sigma^{\varepsilon}_{rr} - \sigma^{\varepsilon}_{\theta\theta}}{r} = 0, \quad \frac{\mathrm{d}\sigma^{\varepsilon}_{r\theta}}{\mathrm{d}r} + 2\frac{\sigma^{\varepsilon}_{r\theta}}{r} = 0, \quad \frac{\mathrm{d}\sigma^{\varepsilon}_{rz}}{\mathrm{d}r} + \frac{\sigma^{\varepsilon}_{rz}}{r} = 0. \tag{76}$$

We assume the following boundary conditions,

$$[\sigma^{\varepsilon}_{rr} \quad \sigma^{\varepsilon}_{r\theta} \quad \sigma^{\varepsilon}_{rz} \quad u^{\varepsilon}_{\theta} \quad u^{\varepsilon}_{z}]_a = [-p_i \quad t_i \quad s_i \quad u_{\theta_i} \quad u_{z_i}], [\sigma^{\varepsilon}_{rr}]_b = [-p_o], \quad p_o > p_i > 0. \tag{77}$$

For the system of equations (75)–(77) we assume that all elastic coefficients are bounded from above and from below by strictly positive constants and that they are allowed to exhibit discontinuities. Moreover, we assume that

$$C^{\varepsilon}_{55}C^{\varepsilon}_{66} - (C^{\varepsilon}_{56})^2 \neq 0. \tag{78}$$

From $(76)_2$ and $(76)_3$ we get

$$\sigma^{\varepsilon}_{r\theta} = t_i\frac{a^2}{r^2}, \quad \sigma^{\varepsilon}_{rz} = s_i\frac{a}{r}, \tag{79}$$

from which obviously

$$\sigma^{h}_{r\theta} = t_i\frac{a^2}{r^2}, \quad \sigma^{h}_{rz} = s_i\frac{a}{r}. \tag{80}$$

Combining (79), $(75)_5$ and $(75)_6$ leads to

$$u^{\varepsilon}_{\theta} = u_{\theta_i}\frac{r}{a} + r\int_a^r \left(\frac{s_i a}{\xi^2}S^{\varepsilon}_{55}(\xi) - \frac{t_i a^2}{\xi^3}S^{\varepsilon}_{56}(\xi)\right)\mathrm{d}\xi, \tag{81}$$

$$u^{\varepsilon}_{z} = u_{z_i} + \int_a^r \left(-\frac{s_i a}{\xi}S^{\varepsilon}_{56}(\xi) + \frac{t_i a^2}{\xi^2}S^{\varepsilon}_{66}(\xi)\right)\mathrm{d}\xi, \tag{82}$$

where

$$S^{\varepsilon}_{55} = \frac{C^{\varepsilon}_{55}}{C^{\varepsilon}_{55}C^{\varepsilon}_{66} - (C^{\varepsilon}_{56})^2}, \quad S^{\varepsilon}_{56} = \frac{C^{\varepsilon}_{56}}{C^{\varepsilon}_{55}C^{\varepsilon}_{66} - (C^{\varepsilon}_{56})^2}, \quad S^{\varepsilon}_{66} = \frac{C^{\varepsilon}_{66}}{C^{\varepsilon}_{55}C^{\varepsilon}_{66} - (C^{\varepsilon}_{56})^2}, \tag{83}$$

which implies that $|u^{\varepsilon}_{\theta}|$, $|u^{\varepsilon}_{z}|$, $|\frac{\mathrm{d}u^{\varepsilon}_{\theta}}{\mathrm{d}r}|$, $|\frac{\mathrm{d}u^{\varepsilon}_{z}}{\mathrm{d}r}|$ are bounded independently of ε. Therefore,

$$u^{\varepsilon}_{\theta} \to u^{h}_{\theta} \text{ in } C(a,b), \quad u^{\varepsilon}_{z} \to u^{h}_{z} \text{ in } C(a,b). \tag{84}$$

From Eqs. $(75)_{1,2}$ and $(76)_1$ we get

$$\frac{\mathrm{d}\sigma^{\varepsilon}_{rr}}{\mathrm{d}r} + \frac{1 - C^{\varepsilon}_{12}/C^{\varepsilon}_{11}}{r}\sigma^{\varepsilon}_{rr} = \frac{C^{\varepsilon}_{11}C^{\varepsilon}_{22} - (C^{\varepsilon}_{12})^2}{r^2 C^{\varepsilon}_{11}}u^{\varepsilon}_{r}, \quad \frac{\mathrm{d}u^{\varepsilon}_{r}}{\mathrm{d}r} + \frac{C^{\varepsilon}_{12}}{rC^{\varepsilon}_{11}}u^{\varepsilon}_{r} = \frac{\sigma^{\varepsilon}_{rr}}{C^{\varepsilon}_{11}}. \tag{85}$$

We make the following physically justifiable assumptions,

$$C^{\varepsilon}_{11}(r) > C^{\varepsilon}_{12}(r), C^{\varepsilon}_{11}(r)C^{\varepsilon}_{22}(r) - (C^{\varepsilon}_{12}(r))^2 > 0, \ \forall r, \quad a \leqslant r \leqslant b. \tag{86}$$

In Appendix B, based on assumptions (86), we verify that $|\sigma^{\varepsilon}_{rr}|$ is bounded, independently of ε. Then, from (B.4) we get that $|u^{\varepsilon}_{r}(a)|$ is bounded too and (B.3) implies that u^{ε}_{r} is bounded in $L^{\infty}(a,b)$. Eq. (85) lead to the conclusion that $\frac{\mathrm{d}\sigma^{\varepsilon}_{rr}}{\mathrm{d}r}$ and $\frac{\mathrm{d}u^{\varepsilon}_{r}}{\mathrm{d}r}$ are bounded in $L^{\infty}(a,b)$. So, following the same lines as in previous sections, we prove that

$$u^{\varepsilon}_{r} \to u^{h}_{r} \text{ in } C(a,b), \quad \sigma^{\varepsilon}_{rr} \to \sigma^{h}_{rr} \text{ in } C(a,b). \tag{87}$$

An interesting observation is that all the quantities for which Tarn and Wang (2001) assumed interfacial continuity conditions are proved to be continuous. Now, we write the system (75) by putting in the right hand side the radial displacement and the stresses which converge strongly,

$$\begin{bmatrix} \frac{du_r^\varepsilon}{dr} \\ \sigma_{\theta\theta}^\varepsilon \\ \sigma_{zz}^\varepsilon \\ \sigma_{z\theta}^\varepsilon \\ \frac{du_z^\varepsilon}{dr} \\ \frac{du_\theta^\varepsilon}{dr} - \frac{u_\theta^\varepsilon}{r} \end{bmatrix} = \begin{bmatrix} \frac{1}{C_{11}^\varepsilon} & -\frac{C_{12}^\varepsilon}{C_{11}^\varepsilon} & 0 & 0 \\ \frac{C_{12}^\varepsilon}{C_{11}^\varepsilon} & C_{22}^\varepsilon - \frac{(C_{12}^\varepsilon)^2}{C_{11}^\varepsilon} & 0 & 0 \\ \frac{C_{13}^\varepsilon}{C_{11}^\varepsilon} & C_{23}^\varepsilon - \frac{C_{12}^\varepsilon C_{13}^\varepsilon}{C_{11}^\varepsilon} & 0 & 0 \\ \frac{C_{14}^\varepsilon}{C_{11}^\varepsilon} & C_{24}^\varepsilon - \frac{C_{12}^\varepsilon C_{14}^\varepsilon}{C_{11}^\varepsilon} & 0 & 0 \\ 0 & 0 & S_{66}^\varepsilon & -S_{56}^\varepsilon 00 - S_{56}^\varepsilon S_{55}^\varepsilon \end{bmatrix} \begin{bmatrix} \sigma_{rr}^\varepsilon \\ \frac{u_r^\varepsilon}{r} \\ \sigma_{rz}^\varepsilon \\ \sigma_{r\theta}^\varepsilon \end{bmatrix}. \tag{88}$$

Then, following the same lines as in previous sections,

$$\sigma_{\theta\theta}^\varepsilon \rightharpoonup \sigma_{\theta\theta}^h \text{ in} L^\infty(a,b) \text{ weakstar},$$
$$\sigma_{zz}^\varepsilon \rightharpoonup \sigma_{zz}^h \text{ in} L^\infty(a,b) \text{ weakstar},$$
$$\sigma_{z\theta}^\varepsilon \rightharpoonup \sigma_{z\theta}^h \text{ in} L^\infty(a,b) \text{ weakstar}.$$

We pass to the limit in (88) to obtain the limit equations of the problem

$$\begin{bmatrix} \frac{du_r^h}{dr} \\ \sigma_{\theta\theta}^h \\ \sigma_{zz}^h \\ \sigma_{z\theta}^h \\ \frac{du_z^h}{dr} \\ \frac{du_\theta^h}{dr} - \frac{u_\theta^h}{r} \end{bmatrix} = \begin{bmatrix} \left\langle \frac{1}{C_{11}^\varepsilon} \right\rangle & -\left\langle \frac{C_{12}^\varepsilon}{C_{11}^\varepsilon} \right\rangle & 0 & 0 \\ \left\langle \frac{C_{12}^\varepsilon}{C_{11}^\varepsilon} \right\rangle & \left\langle C_{22}^\varepsilon - \frac{(C_{12}^\varepsilon)^2}{C_{11}^\varepsilon} \right\rangle & 0 & 0 \\ \left\langle \frac{C_{13}^\varepsilon}{C_{11}^\varepsilon} \right\rangle & \left\langle C_{23}^\varepsilon - \frac{C_{12}^\varepsilon C_{13}^\varepsilon}{C_{11}^\varepsilon} \right\rangle & 0 & 0 \\ \left\langle \frac{C_{14}^\varepsilon}{C_{11}^\varepsilon} \right\rangle & \left\langle C_{24}^\varepsilon - \frac{C_{12}^\varepsilon C_{14}^\varepsilon}{C_{11}^\varepsilon} \right\rangle & 0 & 0 \\ 0 & 0 & \langle S_{66}^\varepsilon \rangle & -\langle S_{56}^\varepsilon \rangle \\ 0 & 0 & -\langle S_{56}^\varepsilon \rangle & \langle S_{55}^\varepsilon \rangle \end{bmatrix} \begin{bmatrix} \sigma_{rr}^h \\ \frac{u_r^h}{r} \\ \sigma_{rz}^h \\ \sigma_{r\theta}^h \end{bmatrix}. \tag{89}$$

By rearranging the system (89), we end up with

$$\begin{bmatrix} \sigma_{rr}^h \\ \sigma_{\theta\theta}^h \\ \sigma_{zz}^h \\ \sigma_{z\theta}^h \\ \sigma_{rz}^h \\ \sigma_{r\theta}^h \end{bmatrix} = \begin{bmatrix} C_{11}^h & C_{12}^h & 0 & 0 \\ C_{12}^h & C_{22}^h & 0 & 0 \\ C_{13}^h & C_{23}^h & 0 & 0 \\ C_{14}^h & C_{24}^h & 0 & 0 \\ 0 & 0 & C_{55}^h & C_{56}^h \\ 0 & 0 & C_{56}^h & C_{66}^h \end{bmatrix} \begin{bmatrix} \frac{du_r^h}{dr} \\ \frac{u_r^h}{r} \\ \frac{du_z^h}{dr} \\ \frac{du_\theta^h}{dr} - \frac{u_\theta^h}{r} \end{bmatrix}, \tag{90}$$

where the elements of the effective tensor of elastic material coefficients are

$$C_{11}^h = \frac{1}{\langle 1/C_{11}^\varepsilon \rangle}, \quad C_{1j}^h = C_{11}^h \left\langle \frac{C_{1j}^\varepsilon}{C_{11}^\varepsilon} \right\rangle, \quad C_{2j}^h = \left\langle \frac{C_{1j}^\varepsilon}{C_{11}^\varepsilon} \right\rangle C_{12}^h + \left\langle C_{2j}^\varepsilon - C_{1j}^\varepsilon \frac{C_{12}^\varepsilon}{C_{11}^\varepsilon} \right\rangle, \quad C_{55}^h = \frac{\langle S_{55}^\varepsilon \rangle}{\langle S_{55}^\varepsilon \rangle \langle S_{66}^\varepsilon \rangle - \langle S_{56}^\varepsilon \rangle^2},$$
$$C_{56}^h = \frac{\langle S_{56}^\varepsilon \rangle}{\langle S_{55}^\varepsilon \rangle \langle S_{66}^\varepsilon \rangle - \langle S_{56}^\varepsilon \rangle^2}, \quad C_{66}^h = \frac{\langle S_{66}^\varepsilon \rangle}{\langle S_{55}^\varepsilon \rangle \langle S_{66}^\varepsilon \rangle - \langle S_{56}^\varepsilon \rangle^2}, \quad j = 2,3,4. \tag{91}$$

5.1. Numerical example: multilayered anisotropic hollow cylinder under pressure

In this example, we consider a hollow cylinder consisting of 200 thin periodic layers, of two cylindrically orthotropic materials. We choose graphite/epoxy laminae as our first material, where the mechanical characteristics are based on Tarn and Wang (2001). The second material is produced by the first one, by 90° rotation around z-axis. The matrix of elastic coefficients of these two materials are

$$\mathbf{C}_1 = \begin{pmatrix} 139.638 & 3.9 & 0 & 0 \\ 3.9 & 15.278 & 0 & 0 \\ 3.9 & 3.294 & 0 & 0 \\ 0 & 0 & 5.86 & 0 \\ 0 & 0 & 0 & 5.86 \end{pmatrix}, \quad \mathbf{C}_2 = \begin{pmatrix} 15.278 & 3.9 & 0 & 0 \\ 3.9 & 139.638 & 0 & 0 \\ 3.294 & 3.9 & 0 & 0 \\ 0 & 0 & 5.86 & 0 \\ 0 & 0 & 0 & 5.86 \end{pmatrix},$$

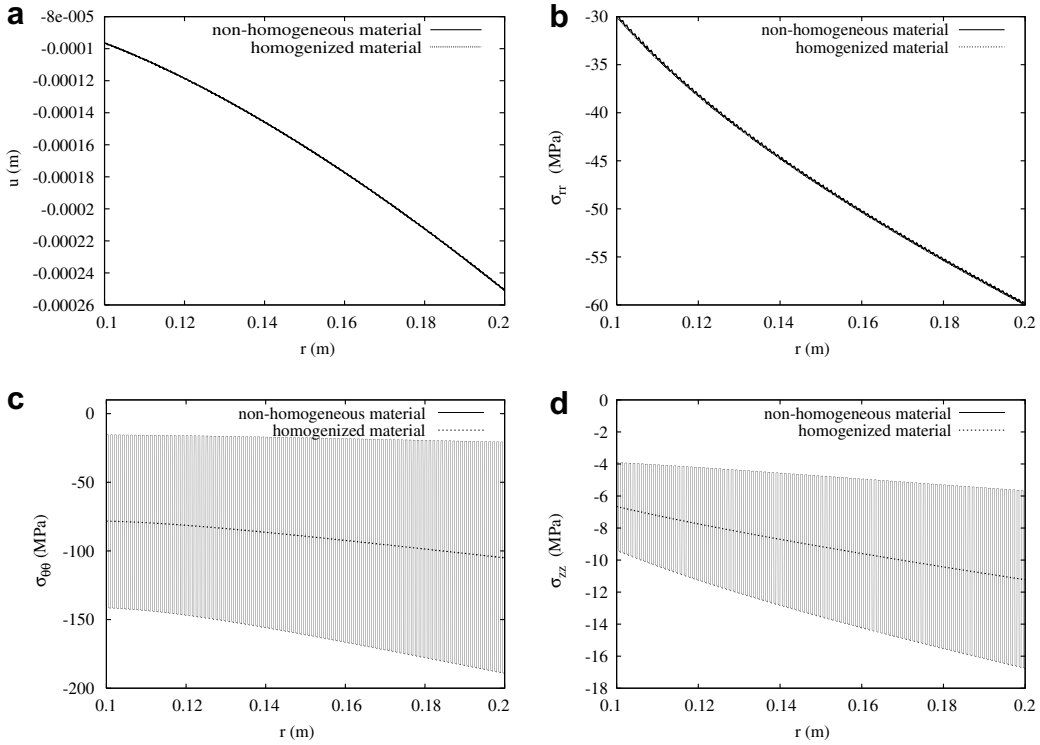

Fig. 9. Radial variation of (a) radial displacement (the curve of the non-homogeneous and the curve of the homogenized coincide with less than 0.5% error), (b) radial stress (the curve of the non-homogeneous and the curve of the homogenized coincide with approximately 1% error), (c) hoop stress and (d) longitudinal stress in the pressurized anisotropic hollow cylinder.

where all coefficients are given in GPa. Under axisymmetric state, the parameters of the homogenized material are given by equations (91), leading to the effective matrix

$$\mathbf{C}_h = \begin{pmatrix} 27.542 & 3.9 & 0 & 0 \\ 3.9 & 77.458 & 0 & 0 \\ 3.354 & 3.597 & 0 & 0 \\ 0 & 0 & 5.86 & 0 \\ 0 & 0 & 0 & 5.86 \end{pmatrix}.$$

In this special case, we observe that the effective coefficients C_{22}^h and C_{23}^h are given by the mean values of the C_{22} and C_{23}-coefficients of the two materials. On the contrary, the effective coefficient C_{11}^h is the inverse of the mean value of the inverse values of the C_{11}-coefficients of the two materials. So, an arbitrary "homogenization", based on the mean values of all material coefficients, is incorrect.

By using the sigmoid function, in order to simulate the discontinuities between the two faces, we can solve the problem of the composite hollow cylinder under pressure, where the radial stress is -30 MPa at the inner surface with radius 0.1 m and -60 MPa at the outer surface with radius 0.2 m. The radial displacement and the radial stress of the non-homogeneous and the homogenized material, shown in Figs. 9a and 9b, are very close. The hoop and the longitudinal stresses are given in Fig. 9c and 9d, respectively. The highest "jump" observed in these stresses is 170 MPa and 11 MPa, respectively.

6. Conclusions

In this paper, we present the theoretical and numerical homogenization of a hollow cylinder made of very dissimilar fine elastic layers. We consider two different sets of boundary conditions, one leading to torsion and one leading to axisymmetric state. We focus on the behavior of a tube made of periodic layers. When the material layers are isotropic, the homogenization induces anisotropic behavior. When the layers of the tube consist of cylindrically anisotropic materials, no other anisotropy is added to the effective properties. Explicit formulas for the effective elastic coefficients are given. All the stress and deformation functions affecting the bonding strength of the layered material are presented. It is worth noticing that the stress field discontinuities in the finely layered cylinders occur in those stress components which are not traction components.

Appendix A

From (23) and (22) we find that ω^ε and X^ε have the following representations

$$\omega^\varepsilon(r) = \omega_a \frac{a^2}{r^2} - \frac{k^2}{r^2}\int_a^r \xi^2 \mu^\varepsilon(\xi) X^\varepsilon(\xi)\mathrm{d}\xi, \tag{A.1}$$

$$X^\varepsilon(r) = X_a \frac{r}{a} + r\int_a^r \frac{1}{\xi}\frac{1}{\mu^\varepsilon(\xi)}\omega^\varepsilon(\xi)\mathrm{d}\xi, \tag{A.2}$$

$$a \leqslant r \leqslant b, \tag{A.3}$$

$$0 < \mu_1 \leqslant \mu^\varepsilon(r) \leqslant \mu_2. \tag{A.4}$$

Combining (A.1) and (A.2) we obtain the representations

$$X^\varepsilon(r) = X_a \frac{r}{a} + r\int_a^r \frac{1}{\xi}\frac{1}{\mu^\varepsilon(\xi)}\left[\frac{a^2}{\xi^2}\omega_a - \frac{k^2}{\xi^2}\int_a^\xi s^2 \mu^\varepsilon(s) X^\varepsilon(s)\mathrm{d}s\right]\mathrm{d}\xi, \tag{A.5}$$

$$\omega^\varepsilon(r) = \omega_a \frac{a^2}{r^2} - \frac{k^2}{r^2}\int_a^r \xi^2 \mu^\varepsilon(\xi)\left[\frac{\xi}{a}X_a + \xi\int_a^\xi \frac{1}{s}\frac{1}{\mu^\varepsilon(s)}\omega^\varepsilon(s)\mathrm{d}s\right]\mathrm{d}\xi. \tag{A.6}$$

From (A.5) we get

$$\frac{\mathrm{d}X^\varepsilon(r)}{\mathrm{d}r} = \frac{1}{a}X_a + \int_a^r \frac{1}{\xi}\frac{1}{\mu^\varepsilon(\xi)}\frac{a^2}{\xi^2}\omega_a\mathrm{d}\xi + \frac{1}{\mu(r)}\frac{a^2}{r^2}\omega_a - \int_a^r \frac{1}{\xi}\frac{1}{\mu(\xi)}\frac{k^2}{\xi^2}\left[\int_a^\xi s^2\mu^\varepsilon(s)X^\varepsilon(s)\mathrm{d}s\right]\mathrm{d}\xi - \frac{1}{\mu(r)}\frac{k^2}{r^2}\int_a^r \xi^2\mu^\varepsilon(\xi)X^\varepsilon(\xi)\mathrm{d}\xi, \tag{A.7}$$

and from (A.6) a corresponding representation for $\frac{\mathrm{d}\omega^\varepsilon(r)}{\mathrm{d}r}$. Using (20) gives that there exists r^* such that $X^\varepsilon(r) > 0$ for $0 < r \leqslant r^*$, so from (A.5) and (A.7) $0 < X^\varepsilon(r) \leqslant c_1$, $0 < \frac{\mathrm{d}X^\varepsilon(r)}{\mathrm{d}r} \leqslant c_2$, $\frac{\mathrm{d}X^\varepsilon(r^*)}{\mathrm{d}r} = 0$, where c_1 and c_2 can be estimated in terms of a, b, X_a ω_a, k and μ_1, independently of ε. After r^* there exist two cases. For large values of k, there exists r^{**} such that $-c_3 < \frac{\mathrm{d}X^\varepsilon(r^{**})}{\mathrm{d}r} < 0$, $X^\varepsilon(r^{**}) = 0$, $X^\varepsilon(r) < X^\varepsilon(r^*)$ for $r^* < r \leqslant r^{**}$, and for $r > r^{**}$, $|X^\varepsilon(r)| \leqslant c_4$, $|\frac{\mathrm{d}X^\varepsilon(r)}{\mathrm{d}r}| \leqslant c_5$, where all constants depend only on a, b, μ_1, μ_2, X_a ω_a, k, independently of ε. For small values of k, $X^\varepsilon(r) > 0$ for all r and a priori estimates independent of ε for $X^\varepsilon(r)$, $\left|\frac{\mathrm{d}X^\varepsilon(r)}{\mathrm{d}r}\right|$ can be obtained as previously. Following the same lines, we can prove that $|\omega^\varepsilon(r)|$ and $\left|\frac{\mathrm{d}\omega^\varepsilon(r)}{\mathrm{d}r}\right|$ are bounded independently of ε.

Appendix B

We put

$$\mathrm{e}^{\int_a^r \frac{1-C_{12}^\varepsilon(\xi)/C_{11}^\varepsilon(\xi)}{\xi}\mathrm{d}\xi} = \phi^\varepsilon(r), \quad \mathrm{e}^{\int_a^r \frac{C_{12}^\varepsilon(\xi)}{\xi C_{11}^\varepsilon(\xi)}\mathrm{d}\xi} = \chi^\varepsilon(r), \quad \frac{C_{11}^\varepsilon(r)C_{22}^\varepsilon(r) - (C_{12}^\varepsilon(r))^2}{r^2 C_{11}^\varepsilon(r)} = \psi^\varepsilon(r) > 0. \tag{B.1}$$

Properties of functions ϕ^ε, χ^ε and ψ^ε, such as the positiveness of ψ^ε, are due to (86). Then, by using the boundary conditions (77), we obtain from equations (85)

$$\sigma_{rr}^\varepsilon(r) = \frac{1}{\phi^\varepsilon(r)}\left(-p_i + \int_a^r \phi^\varepsilon(\xi)\psi^\varepsilon(\xi)u_r^\varepsilon(\xi)\mathrm{d}\xi\right), \tag{B.2}$$

$$u_r^\varepsilon(r) = \frac{1}{\chi^\varepsilon(r)}\left(u_r^\varepsilon(a) + \int_a^r \chi^\varepsilon(\xi)\frac{\sigma_{rr}^\varepsilon(\xi)}{C_{11}^\varepsilon(\xi)}\mathrm{d}\xi\right), \tag{B.3}$$

where $u_r^\varepsilon(a)$ is the undefined value of u_r^ε at $r = a$. Combining equations (B.2) and (B.3) gives

$$\sigma_{rr}^\varepsilon(r) = \frac{1}{\phi^\varepsilon(r)}\left[-p_i + u_r^\varepsilon(a)\int_a^r \zeta^\varepsilon(\xi)\mathrm{d}\xi + \int_a^r \zeta^\varepsilon(\xi)\left(\int_a^\xi \chi^\varepsilon(s)\frac{\sigma_{rr}^\varepsilon(s)}{C_{11}^\varepsilon(s)}\mathrm{d}s\right)\mathrm{d}\xi\right]. \tag{B.4}$$

where

$$\zeta^\varepsilon(r) = \phi^\varepsilon(r)\psi^\varepsilon(r)/\chi^\varepsilon(r) > 0. \tag{B.5}$$

We examine the following cases: A: $u_r^\varepsilon(a) \leqslant 0$. Then, if r^* is the value of r, $a \leqslant r \leqslant b$, where $\sigma_{rr}^\varepsilon(r)$ becomes zero, (B.4) implies that

$$p_i - u_r^\varepsilon(a)\int_a^r \zeta^\varepsilon(\xi)\mathrm{d}\xi = \int_a^{r^*} \zeta^\varepsilon(\xi)\left(\int_a^\xi \chi^\varepsilon(s)\frac{\sigma_{rr}^\varepsilon(s)}{C_{11}^\varepsilon(s)}\mathrm{d}s\right)\mathrm{d}\xi. \tag{B.6}$$

The last equation does not hold, because the left hand side is positive, while the right hand side is negative. So $\sigma_{rr}^\varepsilon(r)$ remains negative for every $a \leqslant r \leqslant b$. Then, (B.4) leads to

$$\begin{aligned}\phi^\varepsilon(r)\sigma_{rr}^\varepsilon(r) &= -p_i + u_r^\varepsilon(a)\int_a^r \zeta^\varepsilon(\xi)\mathrm{d}\xi + \int_a^r \zeta^\varepsilon(\xi)\left(\int_a^\xi \chi^\varepsilon(s)\frac{\sigma_{rr}^\varepsilon(s)}{C_{11}^\varepsilon(s)}\mathrm{d}s\right)\mathrm{d}\xi \\ &\geqslant -p_i + u_r^\varepsilon(a)\int_a^b \zeta^\varepsilon(\xi)\mathrm{d}\xi + \int_a^b \zeta^\varepsilon(\xi)\left(\int_a^b \chi^\varepsilon(s)\frac{\sigma_{rr}^\varepsilon(s)}{C_{11}^\varepsilon(s)}\mathrm{d}s\right)\mathrm{d}\xi = -p_o\phi^\varepsilon(b),\end{aligned} \tag{B.7}$$

which implies that $\sigma_{rr}^\varepsilon \in L^\infty(a,b)$. B: $u_r^\varepsilon(a) > 0$. Then, from (85) we get that $\frac{\mathrm{d}\sigma_{rr}^\varepsilon}{\mathrm{d}r}(a) > 0$ and $\frac{\mathrm{d}u_r^\varepsilon}{\mathrm{d}r}(a) < 0$. We consider three subcases: B_1: There exists r^* such that $u_r^\varepsilon(r^*) = 0$ and $\sigma_{rr}^\varepsilon(r^*) < 0$. In this case, by starting from r^* we are back to case A. B_2: There exists r^* such that $u_r^\varepsilon(r^*) > 0$ and $\sigma_{rr}^\varepsilon(r^*) = 0$. From $(85)_1$ we know that $\frac{\mathrm{d}\sigma_{rr}^\varepsilon}{\mathrm{d}r}(r^*) > 0$, so σ_{rr}^ε continues to increase, while from $(85)_2$, $\frac{\mathrm{d}u_r^\varepsilon}{\mathrm{d}r}(r^*) < 0$, so u_r^ε continues to decrease. Then from (B.2) we get

$$-p_i + \int_a^{r^*} \phi^\varepsilon(\xi)\psi^\varepsilon(\xi)u_r^\varepsilon(\xi)\mathrm{d}\xi = 0.$$

For larger values of r, Eq. (B.2) implies that, as long as u_r^ε remains non-negative, σ_{rr}^ε remains positive. We assume that there exists r^{**} at which $u_r^\varepsilon(r^{**}) = 0$ and $\sigma_{rr}^\varepsilon(r^{**}) > 0$. Then from $(85)_2$ we get that $\frac{\mathrm{d}u_r^\varepsilon}{\mathrm{d}r}(r^{**}) > 0$. In other words $u_r^\varepsilon(r)$, $r \geqslant r^{**}$ increases again, which is not possible. So u_r^ε remains positive, which means that σ_{rr}^ε remains positive. This is in contradiction to the boundary condition at b. So this case is not possible. B_3: There is no r^* such that $u_r^\varepsilon(r^*) = 0$ or $\sigma_{rr}^\varepsilon(r^*) = 0$. Then σ_{rr}^ε and u_r^ε retain their signs and this, from $(85)_1$, implies that $\frac{\mathrm{d}\sigma_{rr}^\varepsilon}{\mathrm{d}r} > 0$ at (a,b). This is not possible, because $\sigma_{rr}(a) = -p_i > \sigma_{rr}(b) = -p_o$ since $p_o > p_i$. B_4: There exists r^* such that $u_r^\varepsilon(r^*) = 0$ and $\sigma_{rr}^\varepsilon(r^*) = 0$. Then, we easily prove that $\sigma_{rr}^\varepsilon(r) = 0$, $\forall r \in [a,b]$, which is impossible.

References

Batra, R.C., Love, B.M., 2006. Determination of effective thermomechanical parameters of a mixture of two elastothermoviscoplastic constituents. International Journal of Plasticity 22, 1026–1061.

Bensoussan, A., Lions, J., Papanicolaou, G., 1978. Asymptotic Methods for Periodic Structures. North Holland.

Boussaa, D., 2006. Optimizing the composition profile of a functionally graded interlayer using a direct transcription method. Computational Mechanics 39 (3), 59–71.

Cavalcante, M., Marques, S., Pindera, M.-J., 2007. Parametric formulation of the finite-volume theory for functionally graded materials-part i: Analysis. Journal of Applied Mechanics-Transactions of the ASME 74 (5), 935–945.

Chatzigeorgiou, G., Charalambakis, N., Kalpakides, V., 2007. Biaxial loading of continuously graded thermoviscoplastic materials. Computational Mechanics 39 (4), 335–355.

Chen, L., Urquhart, E., Pindera, M.-J., 2005. Microstructural effects in multilayers with large moduli contrast loaded by flat punch. AIAA Journal 43 (5), 962–973.

Chen, T., Chung, C.-T., Lin, W.-L., 2000. A revisit of a cylindrically anisotropic tube subjected to pressuring, shearing, torsion, extension and a uniform temperature change. International Journal of Solids and Structures 37, 5143–5159.

Drago, A., Pindera, M.-J., 2007. Micro-macromechanical analysis of heterogeneous materials: macroscopically homogeneous vs periodic microstructures. Composites Science and Technology 67, 1243–1263.

Geymonat, G., Krasucki, F., Marigo, J.-J., 1987a. On the commutativity of limiting processes in the asymptotic theory of composite rods. Comptes Rendus de l' Académie de Sciences de Paris, Série II, Mécanique, Physique, Chimie, Sciences de l'Univers et Sciences de la Terre 305 (4), 225–228.

Geymonat, G., Krasucki, F., Marigo, J.-J., 1987b. Stress distribution in anisotropic elastic composite beams. Recherches de Mathematiques Appliqees 4, 118–133.

Horgan, C., Chan, A., 1999a. The pressurized hollow cylinder or disk problem for functionally graded isotropic linearly elastic materials. Journal of Elasticity 55 (1), 43–59.

Horgan, C., Chan, A., 1999b. The stress response of functionally graded isotropic linearly elastic rotating disks. Journal of Elasticity 55 (1), 219–230.

Murat, F., 1977. H-convergence. Séminaire d'analyse fonctionnelle et numérique de l'Université d'Alger.

Pindera, M.-J., Chen, L., 2007. Microstructural effects in finite multilayers with aligned cracks. Engineering Fracture Mechanics 74 (11), 1697–1718.

Ruhi, M., Angoshtari, A., Naghdabadi, R., 2005. Thermoelastic analysis of thick-walled finite-length cylinders of functionally graded materials. Journal of Thermal Stresses 28, 391–408.

Sanchez-Palencia, E., 1978. Non-homogeneous media and vibration theory. Lecture Notes in Physics, vol. 127. Springer-Verlag.

Seto, T., Nishimura, T., 2004. Study of two-dimensional elasticity on FGM. In: Proceedings of 21st International Congress of Theoretical and Applied Mechanics, Warsaw.

Suquet, P., 1982. Plasticité et homogénéisation. Ph.D. thesis, Université Pierre et Marie Curie.

Tarn, J.-Q., Wang, Y.-M., 2001. Laminated composite tubes under extension, torsion, bending, shearing and pressuring: a state space approach. International Journal of Solids and Structures 38, 9053–9075.

Tarn, J.-Q., 2002a. Exact solutions of a piezoelectric circular tube or bar under extension, torsion, pressuring, shearing, uniform electric loading and temperature change. Proceedings of the Royal Society of London 458, 2349–2367.

Tarn, J.-Q., 2002b. A state space formalism for anisotropic elasticity. part ii: cylindrical anisotropy. International Journal of Solids and Structures 39, 5157–5172.

Tartar, L., 1977. Homogéneisation et compacité par compensation. Cours Peccot, Collège de France.